Cement and Concrete Composites 109 (2020) 103574

Contents lists available at ScienceDirect

Cement and Concrete Composites

journal homepage: http://www.elsevier.com/locate/cemconcomp

The effect of curing temperature on autogenous deformation of fly ash concretes

Anja Estensen Klausen [a,*], Terje Kanstad [a], Øyvind Bjøntegaard [b], Erik J. Sellevold [a]

[a] Norwegian University of Science and Technology (NTNU), Department of Structural Engineering, Richard Birkelandsvei 1a, 7491, Trondheim, Norway
[b] Norwegian Public Roads Administration, Road Directorate, Tunnel and Concrete Section, Abels Gate 5, 7030, Trondheim, Norway

ARTICLE INFO

Keywords:
Concrete
Autogenous deformation
Shrinkage
Temperature
Curing
Fly ash

ABSTRACT

For concrete subjected to restrained conditions, autogenous deformation (AD) and thermal dilation (TD) are the main driving forces behind stress development in the hardening phase. Generally, AD in concrete is modelled by model codes or measured in the laboratory under 20 °C isothermal conditions, and then used as basis for stress calculations under realistic temperature conditions. To evaluate this common simplification, the current study investigated the effect of curing temperature on the AD of a series of fly ash concretes. A comprehensive test program was performed for fly ash concretes subjected to various temperature curing conditions. The model codes and measurements under 20 °C isothermal conditions provided AD developments in the same order of magnitude. However, when subjected to a realistic temperature history during curing, major changes in the AD developments were observed, emphasising that AD must be determined under relevant temperature conditions.

1. Introduction

Hardening phase volume changes in concrete, caused by autogenous deformation (AD) and thermal dilation (TD), are proven to be of considerable importance. If these movements are restrained by the geometry of the concrete structure or from casting joints against adjoining structural parts, stresses will generate in the newly cast concrete and may further lead to cracking. Early age cracking due to AD and TD is likely to be the most common cause of unsightly cracking in concrete, and it may also lead to functionality, durability and economic issues. In addition, AD may also cause other detrimental effects in concrete, e.g. loss of prestress, axial shortening, torsion and gradual widening of existing cracks over time.

AD is primarily a consequence of chemical shrinkage: the absolute volume of hydration products is less than the total volume of the reactants (cement and water). A part of this inner volume loss appears as an external shrinkage which is the AD [1]. The main mechanism behind AD is assumed to be self-desiccation due to reduction in the water saturation as water is consumed by the on-going cement hydration in the concrete, i.e. capillary forces (negative pore water pressure) [2–7]. Volume changes caused by AD are found to be especially predominant in high performance concrete. This is related to the increased degree of self-desiccation caused by the low water/binder ratio and the addition of silica fume [4,6,8–11].

The documented effect of fly ash on AD found in the literature is somewhat contradicting. There has been reported that a partial replacement of cement by fly ash would increase the AD [12], while other studies found a clear tendency of decreasing AD with increasing fly ash replacement under 20 °C isothermal conditions [11,13]. Klausen [14] reported that replacing cement with fly ash (1:1 by weight) by 17% would decrease the AD development considerably. However, increasing the fly ash replacement further from 17% and up to 33% did not seem to affect the AD behaviour under 20 °C isothermal conditions. The opposite observation was reported by Termkhajornkit et al. [15], who found that replacing cement with fly ash by 25% would not affect the AD much, however, increasing the fly ash replacement further from 25% up to 50% would give a considerable decrease in the long-term AD (beyond 10 days).

Despite its complex nature, various attempts to model AD development can be found in the literature: e.g. Ref. [16,17] based on the maturity principle, and [18–20] based on a capillary tension approach. In addition, several standards and guidelines also provide models to describe the AD development, e.g. Eurocode 2, Model Code 2010 and the Japanese Concrete Institute (JCI) guideline [21–23]. AD development can also be determined by laboratory experiments. Such measurements are mainly performed under 20 °C isothermal conditions, and the start

* Corresponding author.
E-mail address: anja.klausen@ntnu.no (A.E. Klausen).

https://doi.org/10.1016/j.cemconcomp.2020.103574
Received 18 January 2019; Received in revised form 26 February 2020; Accepted 27 February 2020
Available online 29 February 2020

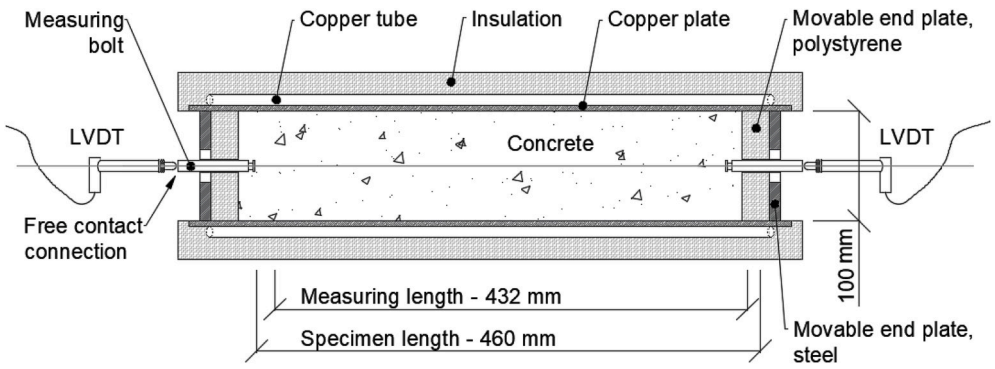

Fig. 1. Dilation rig of the TSTM System, after [34].

time for the deformation measurements is often set to 24 h [24–26].

However, AD development has been found to be strongly influenced by the concrete curing temperature [5,14,17,27–31]. Several of these references concluded that the traditional maturity concept was not applicable to describe the AD development [5,14,28,31]. It is therefore highly questionable if AD models and experiments based on 20 °C isothermal test conditions could accurately describe the AD development taking place under realistic temperature curing conditions.

AD measured under realistic temperature conditions is deduced by subtracting TD from the total measured free deformation. Thus, as described in Ref. [32], the deformation deduced as AD may actually also include some temperature-related mechanisms:

- *Delayed thermal dilation.* Water has a higher CTE value than the other concrete constituents. Thus, after the initial fast expansion due to a temperature increase, a delayed and time-dependent contraction will occur as the induced excess water pressure in filled pores dissipates by flow to the outside or to partly empty pores. This delayed thermal dilation has the opposite direction to the immediate thermal dilation.
- *Thermally induced shrinkage and swelling.* According to thermodynamics, a temperature increase in the concrete will induce an internal redistribution of water from gel pores to capillary pores, caused by the lower entropy of gel water than that of capillary water. This redistribution is expected to lead to a shrinkage, i.e. also the described thermally induced shrinkage and swelling has the opposite direction to the immediate thermal dilation.

Both the above described mechanisms are expected to be "symmetrical", i.e. the opposite effect is expected on cooling. Due to the delayed occurrence, these temperature-induced deformations are usually not counted for by the CTE, but rather included in the deduced AD. This underlines how closely AD and TD are connected, and illustrates how challenging it is to separate these two mechanisms.

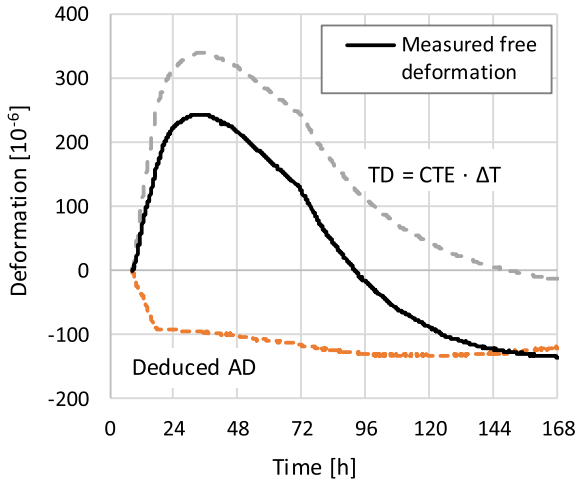

Fig. 2. Measured free deformation, calculated TD (CTE·ΔT) and deduced AD for a concrete specimen subjected to a realistic temperature history.

Over the recent years, a comprehensive experimental test program on fly ash concretes has been performed at NTNU [14,33–35]. The main purpose has been to determine decisive parameters for early age crack assessment. The present paper presents a set of results from this test program: AD measurements on fly ash concretes subjected to 1) 20 °C isothermal temperature curing conditions and 2) realistic temperature curing conditions. Consequently, the current work provides comprehensive experimental data on various concrete mixes and temperature conditions, and thus aims to form a contribution to the ongoing scientific process of understanding the acting mechanisms and developing practical models when it comes to AD of concrete.

2. Experimental set-up

Three different test systems were used for the current AD measurements.

Firstly, a standard test method developed at SINTEF was used to measure 20 °C isothermal long-term AD. In this method, the 100 × 100 × 500 mm specimens were demoulded after 24 h and carefully wrapped in thin plastic sheets and aluminium foil to prevent external drying. The deformation was measured by a manual extensometer over the distance between steel bolts placed centrically in each end. The measurements started at 24 h, and both the deformation and the weight loss was recorded as a part of the standard procedure [25].

The second test method was the Dilation Rig, Fig. 1. The Dilation Rig is the dummy specimen following the Temperature-Stress Testing Machine (TSTM), which is designed to measure the concrete stress development in the hardening phase at a given degree of restraint. In this case, the sum of AD and TD was measured on a 100 × 100 × 460 mm specimen cast directly into a copper form. The Dilation Rig is temperature-controlled: The formwork of copper is surrounded by 5 mm copper pipes with circulating water which is connected to a Julabo FP45 temperature-control unit. During testing, the specimen was isolated against external drying by two layers of plastic as well as aluminium foil. The tests were performed under both 20 °C isothermal conditions and realistic temperature conditions. The length change measurements were initiated approximately 2 h after mixing [14], i.e. before the time of setting.

The third test method was the Free Deformation (FD) System, which consists of seven temperature-controlled rigs of similar type as the Dilation Rig. The tests performed in the FD System were at 20 °C isothermal conditions, and the same procedure as for the Dilation Rig tests was used. The geometry of the FD specimens was the same as for the two previously described methods: prisms with dimensions 100 × 100 × 500mm.

All three test set-ups have been used in parallel for several test

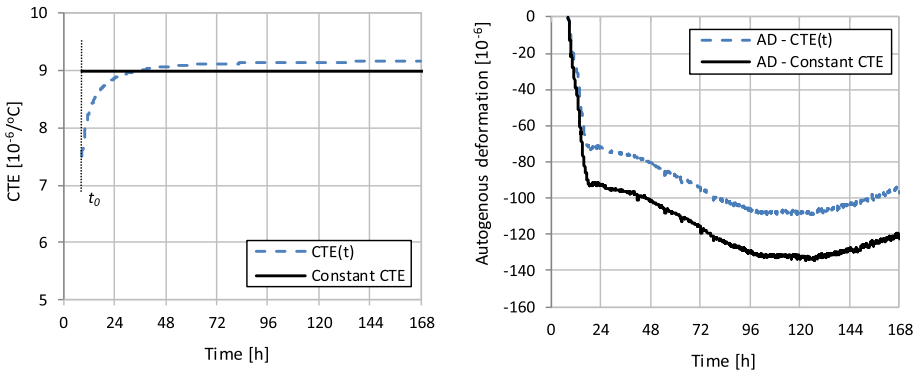

Fig. 3. CTE as a function of time CTE(t) versus a constant CTE (left), and corresponding deduced autogenous deformation (right) for a test with realistic temperature conditions.

programs over the recent years. When compensating for the different start-up time (2 h vs 24 h), all the three test set-ups have shown to give very good agreement (i.e. beyond 24 h). In addition, the Dilation Rig has through a considerable number of tests proven to provide very good reproducibility, both under 20 °C isothermal conditions and under realistic temperature conditions [14,36,37]. For instance, three nominally identical tests performed in the Dilation Rig under realistic temperature conditions gave a standard deviation of only 2.2 and 2.1 μstrain after 48 and 144 h, respectively [14]. Corresponding results for three nominally identical isothermal tests were 4.0 and 3.0 μstrain after 48 and 240 h, respectively [14].

For the tests with a realistic temperature history, the AD development was deduced by subtracting the thermal dilation from the measured total deformation, using the coefficient of thermal expansion (CTE) and the measured temperature development, Fig. 2. In the following, shrinkage is denoted with negative values and expansion is denoted with positive values. The CTE is a complex parameter which varies both with time and moisture content [32]. However, in the current study the often-used simplification of a constant CTE over time was applied. For most of the performed test, the CTE was determined by applying temperature loops at the end of the tests. Based on these results, one average CTE, assumed to be constant over time, was determined for each concrete. This constant CTE approximation will introduce an inaccuracy to the deduced AD. Fig. 3 illustrates the effect on the deduced AD development when using a constant CTE instead of a CTE which varies with time, CTE(t), which is more correct from a fundamental viewpoint. The CTE development over time was estimated by the maturity-based model proposed by Bjøntegaard et al. [38]. The model was applied an assumed curve fitting parameter n_{CTE} of 0.40, an assumed minimum CTE value of $7.5{\cdot}10^{-6}$/°C at the start time for stress development t_0 and a long-term value deduced from the given test. Fig. 3 shows that the simplification of a constant CTE causes an increased contraction very early in the period where the CTEs differ (between t_0 and 48 h). If using the deduced AD in early age crack calculations, the simplification of a constant CTE would only have a limited influence on the stress development, as the early difference between the AD curves occurs in a phase where the E-modulus is still rather low. Also, in most cases TD is still the main contributor when it comes to early age deformation, and thus a small incorrectness in the AD will only constitute a small part of the total free deformation (TD + AD). The main point is therefore that the currently used constant CTE will slightly overestimate (in form of an early parallel displacement) the real AD development, but it will not change the basic characteristics of the resulting AD. Under isothermal conditions and for the realistic temperature tests beyond two weeks (when the temperature is constant), the AD is found directly from the measurements, and thus does not depend on the CTE.

Table 1
Concrete composition and mechanical properties at 28 days.

Materials	*ANL FA17*	*ANL FA33*	*ANL FA45*
Concrete composition [kg/m³]			
Cement	365.3	284.3	229.8
FA_{cem} (FA included in the cement)	60.6	47.2	38.1
FA_{added} (additional added FA)	0.0	71.1	118.5
Silica fume	18.3	17.6	17.4
Free water	160.7	156.2	153.3
Sand 0-2	201.1	201.1	201.1
Sand 0-8	740.2	740.2	740.2
Sand 4-8	275.0	275.0	275.0
Gravel 8-16	614.1	614.1	614.1
Plasticizer	2.01	1.56	1.56
Measured values: fresh concrete			
Natural air content [%]	2.3	2.3	2.0
Density [kg/m³]	2400	2370	2380
Slump [mm]	175	180	205
Binder composition (ratio)			
Total FA-content, FA/(cem + FA)	17%	33%	45%
Silica fume-content, Silica/(cem + FA)	5%	5%	5%
w/b, $k_{FA\_added} = 1.0$[a]	0.40	0.40	0.40
(w/b, $k_{FA\_added} = 0.7$[a])	(0.40)	(0.42)	(0.44)
Mechanical properties			
$f_{c28,\ cube}$ [MPa]	71.2	53.6	45.3
f_{t28} [MPa]	3.55	3.05	3.02
E_{c28} [GPa]	30.55	27.80	24.88
t_0 [h]	9.5	12.0	13.0

[a] k_{FA} = efficiency factor.

3. Materials and experimental program

Test results for three concretes are presented in the following: ANL FA17 (17% FA), ANL FA33 (33% FA) and ANL FA45 (45% FA), where the total fly ash content is given in parenthesis as percentage by weight of cement and fly ash content. The detailed concrete composition and mechanical properties at 28 days are given in Table 1. It should be noted that the differences in compressive cube strengths between the investigated concretes were found to decrease over time, probably due to the correlation between long-term property development and fly ash content. Between 28 and 91 days, the increase in compressive cube strength for ANL FA33 and ANL FA45 was 8.4 MPa (15%) and 15.6 MPa (34%), respectively [14].

The concretes were made with Portland fly ash cement CEM II/A-V 42.5 N "*Norcem Anlegg FA*" (ANL FA17), a water-to-binder ratio of 0.4 and a cement paste volume of 292 l/m³. The fly ash content was increased by replacing cement with fly ash 1:1 by weight, while keeping the water-to-binder ratio and the cement paste volume constant. The chemical and physical properties of the cement and FA are described in Ref. [13,14], respectively. The FA has a fineness (Blaine) of 388 m²/kg and a specific weight of 2200 kg/m³. All concretes contain 5% silica

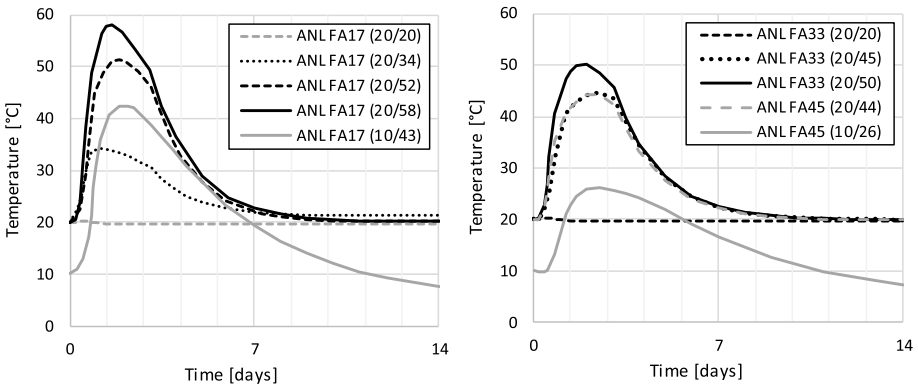

Fig. 4. Temperature histories used for the TSTM tests: ANL FA17 (left) ANL FA33 and ANL FA45 (right).

Table 2
Test program.

Test method and concrete	No of tests	T_{ini} [°C]	T_{max} [°C]	ΔT_{max} [°C]	Duration [Weeks]
SINTEF-method					
ANL FA17	2	20	20	0	30 ->
FD-System					
ANL FA17	3	20	20	0	5.5
Dilation Rig					
ANL FA17	4	20	20	0	2–6
ANL FA17	1	20	34	14	1.5
ANL FA17	1	20	52	32	1.5
ANL FA17	1	20	58	38	2.5
ANL FA17	1	10	43	33	3
ANL FA33	1	20	20	0	4
ANL FA33	2	20	45	25	6.5
ANL FA33	1	20	50	30	2.5
ANL FA45	1	20	44	24	8
ANL FA45	1	10	26	16	12

fume (by weight of cement + FA). The currently used mix design, including FA- and silica fume content, was chosen based on common practice in the Norwegian concrete industry as well as requirements found in Norwegian Model Codes and handbooks.

The test program includes three concretes and various temperature histories, and the following notation has been used to identify concrete and temperature history: "*Concrete name, (T_{ini}/T_{max}x)*", where T_{ini} is the initial temperature of the fresh concrete and T_{max} is the maximum concrete temperature during testing. The maximum temperature increase during the hardening phase was defined as $\Delta T_{max} = T_{max} - T_{ini}$.

While half of the presented AD tests were performed under 20 °C isothermal conditions, the other half were subjected to various semi-adiabatic curing conditions, i.e. the concrete specimens were subjected to a realistic temperature history during testing. Each concrete was subjected to its own semi-adiabatic temperature history representing a section of an 800-mm-thick wall [14]. These temperature histories were determined from the program CrackTeSt COIN [39], using calorimetric heat development test results for each concrete and the geometry of the wall. For each concrete, two temperature histories were calculated representing: 1) Norwegian summer conditions: ANL FA17 (20/58), ANL FA33 (20/50) and ANL FA45 (20/44) and 2) Norwegian winter conditions: ANL FA17 (10/43) and ANL FA45 (10/26). For comparison reasons, some tests with alternative realistic temperature histories were also run: ANL FA17 (20/34), ANL FA17 (20/52) and ANL FA33 (20/45). The temperature histories used for the TSTM tests are presented in Fig. 4.

AD developments of the current concretes were measured by the three described test set-ups: The SINTEF-method, the FD-System and the Dilation Rig. The test program is given in Table 2. The AD curves measured in the FD-System and the Dilation Rig were zeroed at the start time for stress development t_0 as determined in Ref. [14], see Table 1. The start time for stress development, t_0, is defined as the time at which the E-modulus reaches values so that the occurring volume changes can produce measurable stresses. Hence, at t_0, both strength and stiffness are defined to be zero, and from this point they start to develop significant values. The AD development measured by the SINTEF-method, on the other hand, start at 24 h as defined in the test procedure.

Table 3
AD model parameters for ANL FA17 (20/20).

Eurocode 2			***fib*** Model Code 2010			The JCI guideline		
f_{ck}	[MPa]	50	f_{cm}	[MPa]	58	T_{max}	[°C]	58.3
			α_{bs}	[−]	700	$t_{e,set}$	[Days]	0.40
						w/c	[−]	0.40
						η_c	[−]	0.85

4. Code-type material models

The measured AD developments were compared with the Code-type models included in the present version of Eurocode 2 (EC2) [21], ***fib*** Model Code 2010 (MC2010) [22] as well as the Japanese Concrete Institute (JCI) guideline [23]. These three AD-models are based on different parameters: The EC2-model depends on compressive strength f_{ck} only. The MC2010-model depends on the mean compressive strength f_{cm} and the cement type α_{bs}, while the JCI-model is based on the maximum concrete temperature T_{max}, the water-to-cement ratio w/c, the initial setting time $t_{e,set}$ and a parameter representing the cement type η_c. The parameters used for the current AD estimations are presented in Table 3. For both the EC2-model and the MC2010-model, the AD development start at time zero. The JCI-model, on the other hand, defines a start time for AD-development at $t = t_{e,set}$.

AD development determined by the above presented models are presented in Fig. 5, where negative values represent shrinkage. The curves are based on 20 °C isothermal curing conditions and properties representing the ANL FA17 concrete. The modelled AD curves are quite similar in a short-time perspective, Fig. 5 (left). However, while the curves estimated from EC2 and MC2010 flattens out after approximately one year, the AD development modelled from the JCI guideline continues to increase gradually over the next six years Fig. 5 (right). This long-term AD development will not affect early age crack assessment, however, it could be decisive for certain long-term calculations, like for instance crack width calculations.

5. Test results and discussion

AD test results for ANL FA17 under 20 °C isothermal temperature conditions are presented in Fig. 6, where shrinkage is denoted with negative values and expansion is denoted with positive values. The

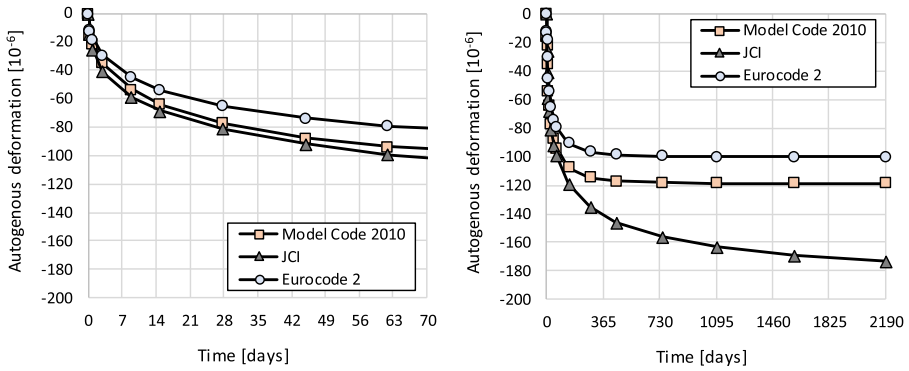

Fig. 5. Modelled AD development for ANL FA17, 20 °C isothermal conditions, 10 weeks (left) 6 years (right).

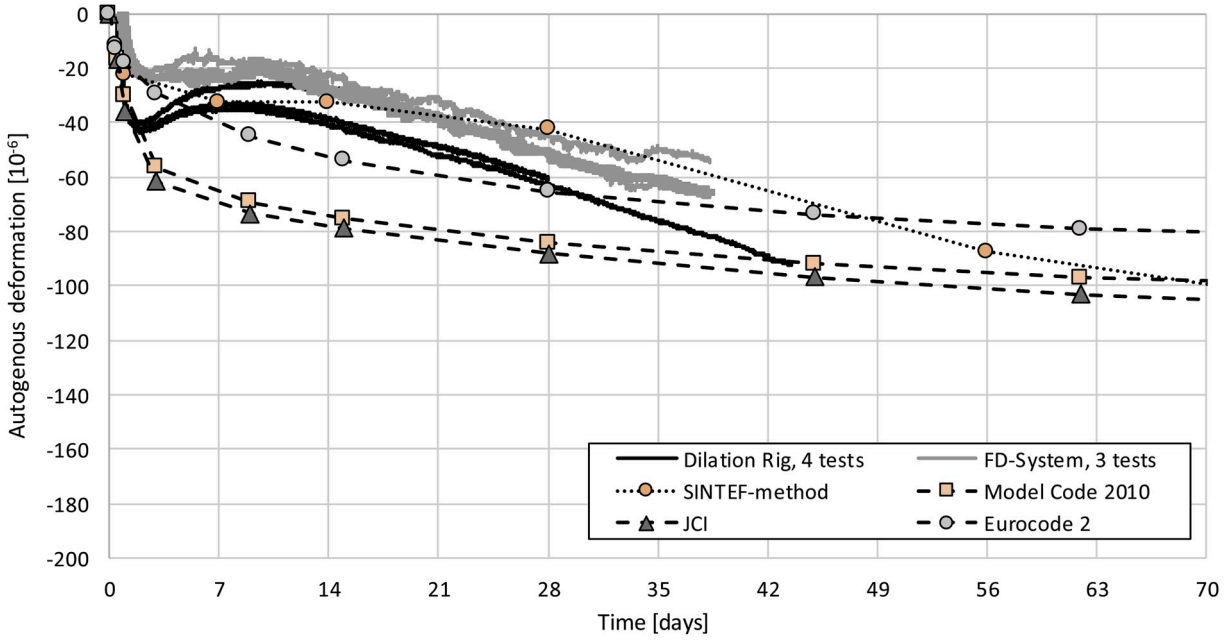

Fig. 6. Autogenous deformation for ANL FA17 under 20 °C isothermal conditions. The measured AD-curves are zeroed at t_0 = 9.5 h.

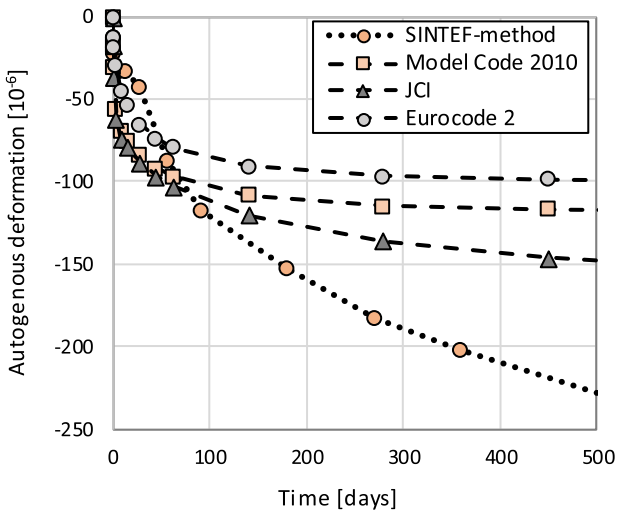

Fig. 7. Measured AD versus modelled AD, ANL FA17 under 20 °C isothermal conditions.

figure shows 4 tests performed in the Dilation Rig, 3 tests performed in the FD-System and the average of 2 tests measured with the SINTEF-method. The figure also presents modelled AD curves for the given concrete. The SINTEF-method has a later measurement start-up than the other test methods. For comparison reasons, this curve was shifted down to match with the other two sets at 24 hours. By allowing for this shift, all three test set-ups were found to give very good agreement. Prior to approximately 35 days, the AD modelled by EC2 is in the same order of magnitude as the measured AD. However, while the models provide a continuous shrinkage, the measurements show an autogenous expansion between 2 and 8 days. Similar expansive behaviour has also been seen in other studies [5,15,28], and different hydration related mechanisms have been proposed as plausible explanations, e.g. ettringite formation and disjoining pressure [6]. There is however no clear consensus in the literature regarding the cause for such expansive behaviour, and further research is required. Beyond 35 days, the AD modelled by EC2 underestimates the measured AD development as the measured AD continues to develop at a higher rate than suggested by the model.

The 20 °C isothermal tests performed with the SINTEF-method are still running at the present time. When compensating for the different start-up time, the measured AD surpassed the EC2-model at approximately 49 days, the JCI-model at approximately 75 days, and it continues to develop at a much higher rate than the models, see Fig. 7. In

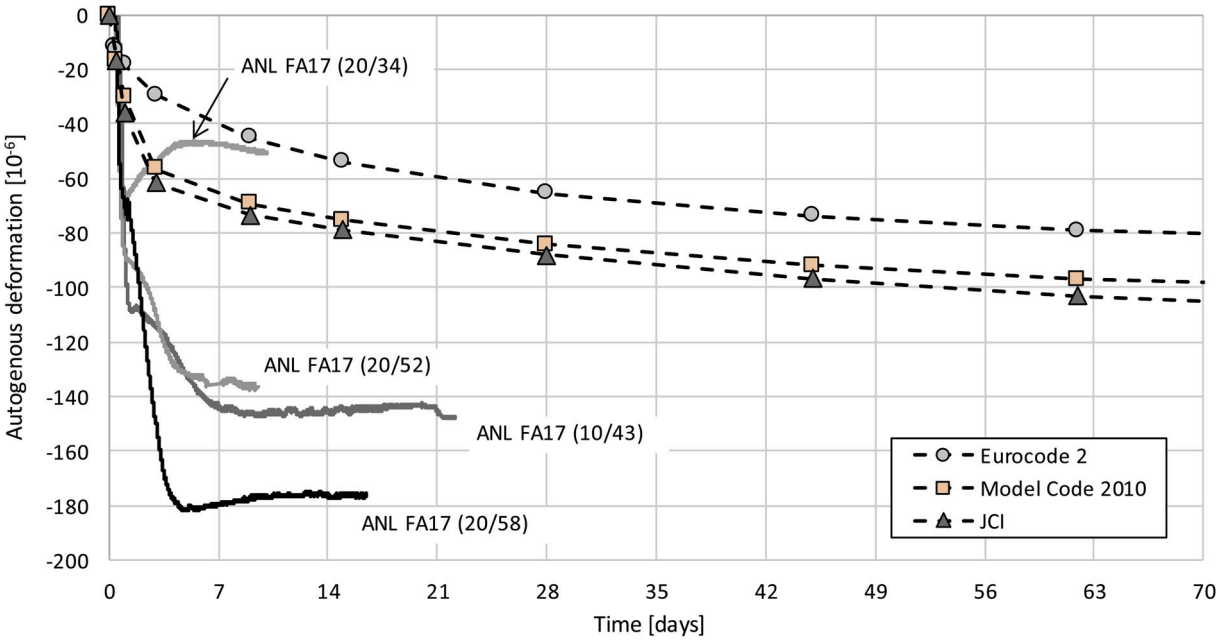

Fig. 8. Autogenous deformation, realistic temperature conditions, ANL FA17. The measured AD-curves are zeroed at t_0 = 9.5 h.

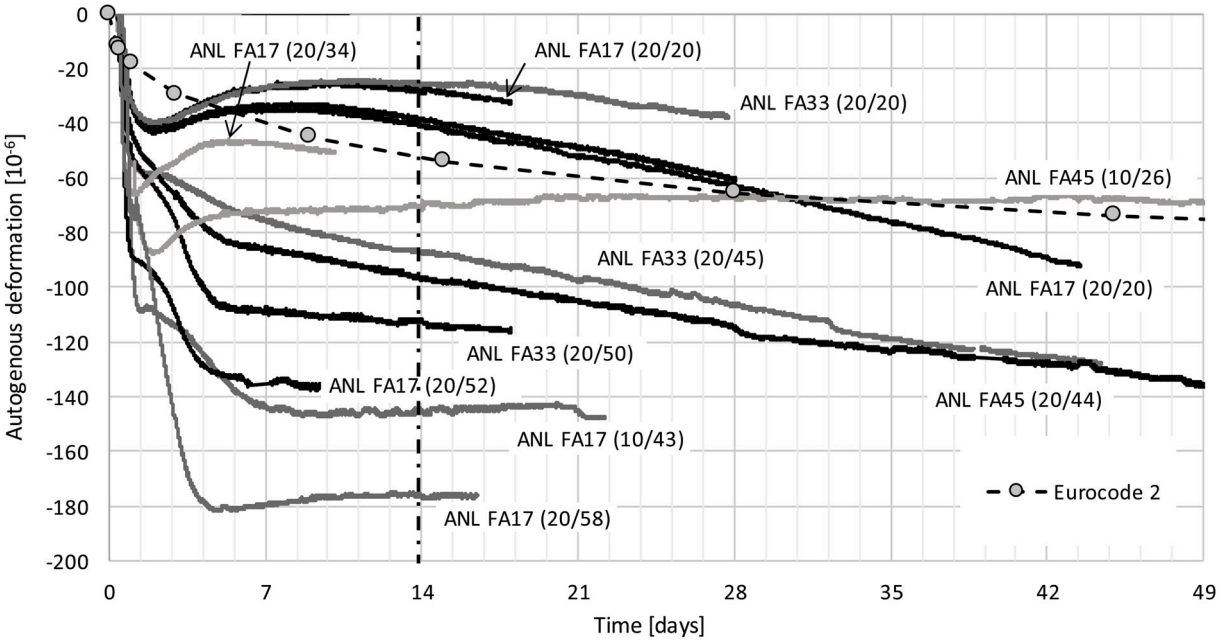

Fig. 9. Autogenous deformation, ANL FA17, ANL FA33 and ANL FA45. The measured AD-curves are zeroed at t_0.

other words, the models considerably underestimate the long-term AD development for ANL FA17.

The AD developments measured for ANL FA17 subjected to various realistic temperature conditions during curing are presented in Fig. 8. The temperature histories applied during testing are shown in Fig. 3. The AD developments deduced from realistic temperature tests are fundamentally different from the corresponding AD obtained under 20 °C curing conditions in that the AD development is much higher. In practice, a project measuring AD development by the SINTEF-method would probably ignore the late start-up at 24 h (i.e. ignore the loss of data prior to 24 h) and use the measured AD values directly for crack risk estimations (i.e. not include the AD development prior to 24 h). At 14 days, which is a quite relevant period for crack risk calculations, the AD measured by the SINTEF-method (= 10 $\mu\varepsilon$) is only 5.6% of the AD measured in the realistic temperature test in the Dilation Rig having a temperature increase ΔT_{max} of 38 °C (= 178 $\mu\varepsilon$) (the latter test includes AD development between t_0 and 24 h). Similarly, the EC2-model estimates an AD of 51 $\mu\varepsilon$ at 14 days, which is 28.7% of the AD obtained from the realistic temperature tests. Consequently, using isothermal measurements or model codes to predict AD under realistic conditions could lead to enormous underestimations of the volume changes, and further to large errors in corresponding stress calculations.

Fig. 9 presents AD curves measured for ANL FA17, ANL FA33 and ANL FA45 when subjected to both 20 °C isothermal and various realistic temperature curing conditions. The figure shows quite similar results for the concretes subjected to 20 °C isothermal conditions, independently of

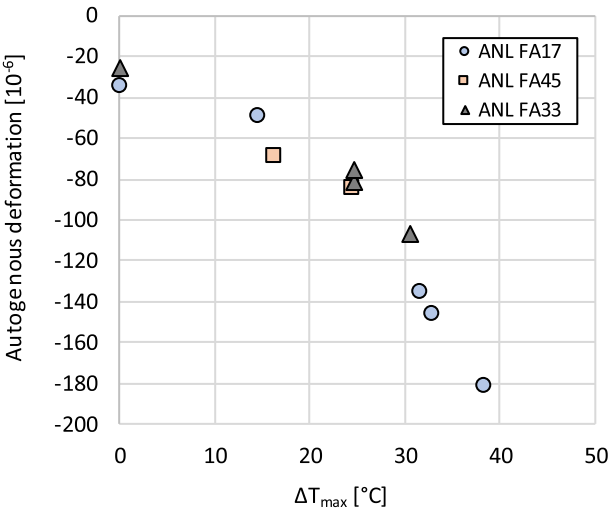

Fig. 10. Autogenous deformation at 336 h of maturity versus maximum temperature increase.

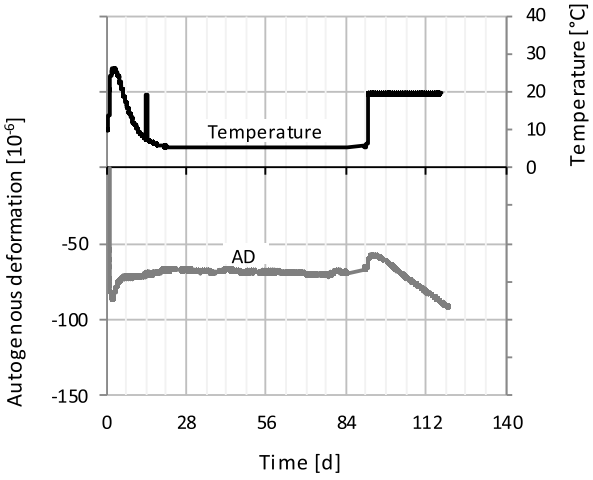

Fig. 11. Autogenous deformation for ANL FA45 (10/26) subjected to winter conditions and 5 °C isothermal temperatures for 13 weeks, followed by 20 °C isothermal temperature conditions for 4 weeks.

the fly ash content. For the realistic temperature tests, the total AD development over the first 14 days (336 h) was systematically increasing with increasing ΔT_{max} regardless of the fly ash content. This systematic relation between AD and ΔT_{max} is clearly illustrated in Fig. 10, which shows deduced AD at 336 maturity hours versus ΔT_{max}. However, beyond 336 h, the given AD curves showed various behaviour and the relation between AD and ΔT_{max} was no longer as systematic.

A rapid increase in AD was observed between t_0 and T_{max} for the realistic temperature tests, which is in accordance with other studies [5,11,15,19]. This initial rapid AD contraction also includes the previously described delayed thermal deformations which are not counted for by the CTE (delayed thermal dilation and thermally induced shrinkage). Also the currently applied simplification of a constant CTE will cause an early increased contraction, but not nearly enough to alone explain the initial very large rapid AD contraction.

Between T_{max} and approximately 2 weeks, i.e. the cooling phase, the AD contraction slowed down, or in some tests even turned into an expansion. This may be caused by delayed thermal deformations, which in this phase occurs as an expansion, and/or by the previously mentioned expansive mechanisms occurring during the hydration phase, e.g. ettringite formation and disjoining pressure. The AD behaviour in the cooling phase seemed to vary with ΔT_{max}. While AD for the concretes subjected to a ΔT_{max} lower than 20 °C occurred as an expansion, the AD for tests with a ΔT_{max} higher than 20 °C occurred as a contraction which was increasing with increasing ΔT_{max}. It should be noted that ettringite formation has been found to decrease with increasing curing temperature [40].

To further elaborate the temperature effects on AD, the temperature in the test ANL FA45 (10/26) was increased to 20 °C after 11 weeks with 5 °C isothermal conditions and a constant AD, (i.e. no AD development which was probably caused by reduced reactivity due to the low temperature). It was found that the temperature increase (+15 °C over 12 h) initiated a revival of the AD development. During the 4 following weeks at 20 °C, i.e. until the test was ended, an AD development of −10 $\mu\varepsilon$ per week was measured (i.e. 40 $\mu\varepsilon$ and continuing), Fig. 11. This rate was the same AD development rate as seen for ANL FA45 (20/44) under 20 °C isothermal conditions (i.e. beyond 2 weeks). This result underlines once again the complex nature of AD.

While the AD development was found to depend strongly on the temperature increase during testing, the fly ash content did not seem to affect the AD behaviour nearly as much. However, for a given structural element, an increasing fly ash content would lead to a reduced maximum curing temperature, and according to the present observations, this would further lead to a reduced AD. An increasing amount of fly ash would thus reduce both AD and TD. Such a reduction is beneficial when it comes to the early age cracking risk, but this must be seen in combination with the corresponding reduction in strength with increasing fly ash content. It should also be noted that the investigated concretes have very different compressive strengths, and are thus not necessary realistic alternatives in a given situation. The differences in compressive strengths between the investigated concretes were however found to decrease over time, probably due to the correlation between long-term property development and fly ash content [14].

6. Summary and conclusion

- For the investigated fly ash concretes, a realistic temperature regime during curing was found to have a major effect on the AD development: The AD was systematically increasing with increasing temperature increase ΔT_{max} during curing (i.e. more massive structures will develop more AD during the hardening phase).
- For all investigated concretes, AD obtained under 20 °C isothermal conditions appeared to be fundamentally different from the corresponding AD deduced from realistic temperature tests. Using isothermal values for AD under realistic conditions will lead to totally unrealistic underestimations of the volume changes, and thus also to the corresponding tensile stress generation obtained by simulation. From this follows that for the currently investigated concretes, AD under realistic temperature conditions could not be modelled and predicted based on 20 °C isothermal test results and the maturity principle, but must be determined from a test using a temperature history as realistic as possible for the actual case/structure.
- An increasing fly ash content will lead to a reduced maximum curing temperature, and according to the present observations, this would further lead to a reduced AD for the investigated fly ash concretes. An increasing amount of fly ash would thus reduce both AD and TD. Such a reduction alone would be beneficial when it comes to the early age cracking risk, but must be seen in combination with the corresponding reduction in strength with increasing fly ash content.
- Results from the present study strongly suggests that AD should be measured under realistic temperature conditions, and that the measurements should start at the start time for stress development t_0 at the latest.

Declaration of competing interest

The current publication is based on the Ph.D. thesis "Early age crack assessment of concrete structures, experimental determination of decisive parameters" by Klausen [14].

The authors declare that they have no conflict of interest.

Acknowledgements

The article is based on work performed in the User-driven Research-based Innovation project DaCS (Durable advanced Concrete Solutions, 2015–2019, funded by the Norwegian Research Council, grantnumber 245645) in addition to COIN (Concrete Innovation Centre, 2007–2014, www.sintef.no/en/projects/coin/coinp, a Centre for Research-based Innovation established by the Research Council of Norway).

References

[1] C.G. Lynam, Growth and Movement in Portland Cement Concrete, Oxford University Press, London, England, 1934.
[2] A. Radocea, A Study on the Mechanism of Plastic Shrinkage of Cement-Based Materials, PhD Thesis, Chalmers University of Technology, Göteborg, Sweden, 1992.
[3] H. Justnes, A.V. Gemert, F. Verboven, E.J. Sellevold, Total and external chemical shrinkage of low w/c ratio cement pastes, Adv. Cement Res. 8 (31) (1996) 121–126, https://doi.org/10.1680/adcr.1996.8.31.121.
[4] O.M. Jensen, P.F. Hansen, Autogenous deformation and change of the relative humidity in silica fume-modified cement paste, ACI Mater. J. 6 (93) (1996) 539–543.
[5] Ø. Bjøntegaard, Thermal Dilation and Autogenous Deformation as Driving Forces to Self-Induced Stresses in High Performance Concrete, PhD Thesis, Norwegian University of Science and Technology (NTNU), Trondheim, Norway, 1999, ISBN 82-7984-002-8.
[6] P. Lura, Autogenous Deformation and Internal Curing of Concrete, PhD Thesis, Delft University of Technology, Netherlands, 2003.
[7] Ø. Bjøntegaard, Basis for and Practical Approaches to Stress Calculations and Crack Risk Estimation in Hardening Concrete Structures - State of the Art, COIN Project Report 31, Trondheim, Norway, 2011. https://www.sintefbok.no/book/index/1012. (Accessed 26 February 2020).
[8] E. Sellevold, D.H. Bager, E.K. Jensen, T. Knudsen, Silica fume cement paste - hydration and pore structure, in: O.E. Gjørv, K.E. Løland (Eds.), Condensed Silica Fume in Concrete, Division of Building Materials, Norwegian University of Science and Technology, Trondheim, Norway, 1982.
[9] Sellevold, et al., Condensed Silica Fume in Concrete. FIP State of the Art Report, Thomas Telford, London, UK, 1988. ISBN 0 7277 1373 6.
[10] O.M. Jensen, P.F. Hansen, A dilatometer for measuring autogenous deformation in hardening Portland cement paste, Mater. Struct. 28 (1995) 406–409, https://doi.org/10.1007/BF02473076.
[11] H.K. Lee, K.M. Lee, B.G. Kim, Autogenous shrinkage of high-performance concrete containing fly ash, Mag. Concr. Res. 55 (2003) 507–515, https://doi.org/10.1680/macr.2003.55.6.507.
[12] M.L. Sennour, R.L. Carrasquillo, Creep and Shrinkage Properties in Concrete Containing Fly Ash, 1989. Austin, Texas.
[13] Ø. Bjøntegaard, K.O. Kjellsen, Property Development and Cracking Tendency in Hardening Concrete: Effect of Cement Type and Fly Ash Content, COIN Project Report 40, 2012. Trondheim, Norway, https://sintefbok.no/book/index/1021. (Accessed 26 February 2020).
[14] A.E. Klausen, Early Age Crack Assessment of Concrete Structures, Experimental Determination of Decisive Parameters, PhD Thesis, Norwegian University of Science and Technology (NTNU), Trondheim, Norway, 2016, https://ntnuopen.ntnu.no/ntnu-xmlui/handle/11250/2430293. (Accessed 26 February 2020).
[15] P. Termkhajornkit, T. Nawa, M. Nakai, T. Saito, Effect of fly ash on autogenous shrinkage, Cement Concr. Res. 35 (2005) 473–482, https://doi.org/10.1016/j.cemconres.2004.07.010.
[16] H. Hedlund, Hardening Concrete, Measurements and Evaluation of Non-elastic Deformation and Associated Restraint Stresses, PhD Thesis, Luleå University of Technology, Sweden, 2000.
[17] H. Hedlund, J.-E. Jonasson, Temperature Effect on Autogenous Deformation. Measurements and Modelling of Thermal and Moisture Related Deformation and Stress, IPACS report, Sweden, 2001.
[18] E.A.B. Koenders, Simulation of Volume Changes in Hardening Cement-Based Materials, PhD Thesis, Delft University of Technology, Netherlands, 1997.
[19] P. Lura, O.M. Jensen, K.v. Breugel, Autogenous shrinkage in high-performance cement paste: an evaluation of basic mechanisms, Cement Concr. Res. 33 (2003) 223–232, https://doi.org/10.1016/S0008-8846(02)00890-6.
[20] F. Grondin, M. Bouasker, P. Mounanga, A. Khelidj, A. Perronnet, Physico-chemical deformations of solidifying cementitious systems: multiscale modelling, Mater. Struct. 43 (2010) 151–165, https://doi.org/10.1617/s11527-009-9477-z.
[21] NS-EN 1992-1-1:2004+NA:2008, Eurocode 2: Design of Concrete Structures, Part 1-1: General Rules and Rules for Buildings, Norsk Standard, 2004.
[22] fib, Model Code for Concrete Structures, Berlin, Germany, 2010, 2010, ISBN 978-3-433-03061-5.
[23] Japan Concrete Institute (JCI), JCI Guidelines for Control of Cracking of Mass Concrete, Tokyo, Japan, 2008.
[24] R.I. Gilbert, A. Castel, I. Khan, W. South, J. Mohammadi, An experimental study of autogenous and drying shrinkage, in: D. Hordijk, M. Luković (Eds.), High Tech Concrete: where Technology and Engineering Meet, Springer, Cham, Online, 2018, ISBN 978-3-319-59471-2.
[25] SINTEF Building and Infrastructure, KS 140504-521 Uttørkings- Og Autogent Svinn for Herdet Betong (In English: Drying Shrinkage and Autogenous Deformation of Concrete), SINTEF Internal Procedure, 2017. Trondheim, Norway.
[26] CEN/TC 104, DRAFT: prEN 12390-16 Testing Hardened Concrete - Part 16: Determination of the Shrinkage of Concrete, 2018.
[27] I.E. Houk, O.E. Borge, D.L. Houghton, Studies of autogenous volume change in concrete for Dworshak Dam, J. Am. Concr. Inst. 66 (1969) 560–568.
[28] O.M. Jensen, P.F. Hansen, Influence of temperature on autogenous deformation and relative humidity change in hardening cement paste, Cement Concr. Res. 29 (1999) 567–575, https://doi.org/10.1016/S0008-8846(99)00021-6.
[29] Ø. Bjøntegaard, T.A. Hammer, E.J. Sellevold, On the measurement of free deformation of early age cement paste and concrete, Cement Concr. Compos. 26 (2004) 427–435, https://doi.org/10.1016/S0958-9465(03)00065-9.
[30] G.-Y. Kim, E.-B. Lee, J.-S. Nam, K.-M. Koo, Analysis of hydration heat and autogenous shrinkage of high-strength mass concrete, Mag. Concr. Res. 63 (2011) 377–389, https://doi.org/10.1680/macr.9.00106.
[31] Ø. Bjøntegaard, E.J. Sellevold, Thermal dilation-autogenous shrinkage: how to separate? in: E.-i. Tazawa (Ed.), International Workshop on Autogenous Shrinkage of Concrete JCI, Hiroshima, Japan, 1998, pp. 245–256.
[32] E.J. Sellevold, Ø. Bjøntegaard, Coefficient of thermal expansion of cement paste and concrete: mechanisms of moisture interaction, Mater. Struct. 39 (2006) 809–815, https://doi.org/10.1617/s11527-006-9086-z.
[33] A.E. Klausen, T. Kanstad, Ø. Bjøntegaard, E.J. Sellevold, The effect of realistic curing temperature on the strength and E-modulus of concrete, Mater. Struct. 51 (2018) 168, https://doi.org/10.1617/s11527-018-1299-4.
[34] A.E. Klausen, T. Kanstad, Ø. Bjøntegaard, E.J. Sellevold, Comparison of tensile and compressive creep of fly ash concretes in the hardening phase, Cement Concr. Res. 95 (2017) 188–194, https://doi.org/10.1016/j.cemconres.2017.02.018.
[35] A.E. Klausen, T. Kanstad, Ø. Bjøntegaard, Hardening concrete exposed to realistic curing temperature regimes and restraint conditions – advanced testing and design methodology, Adv. Mater. Sci. Eng. (2019), https://doi.org/10.1155/2019/9071034. Article ID 9071034.
[36] A.E. Klausen, T. Kanstad, Ø. Bjøntegaard, Updated temperature-stress-testing-machine (TSTM): introductory tests, calculations and verification, in: Proceedings of the XXII Nordic Concrete Research Symposium, Norsk Betongforening Reykjavik, Iceland, 2014, pp. 127–130.
[37] A.E. Klausen, T. Kanstad, Ø. Bjøntegaard, Updated Temperature-Stress Testing Machine (TSTM): introductory tests, calculations, verification and investigation of variable fly ash content, in: Proceedings of CONCREEP 10, Vienna, Austria, 2015, https://doi.org/10.1061/9780784479346.086.
[38] Ø. Bjøntegaard, E.J. Sellevold, Effects of Silica Fume and Temperature on Autogenous Deformation of High Performance Concrete, vol. 220, ACI, Special Publication, 2004, pp. 125–140.
[39] JEJMS Concrete AB, CrackTeSt COIN, Luleå, Sweden, 2009-2012.
[40] K. De Weerdt, M.B. Haha, G.L. Saout, K.O. Kjellsen, H. Justnes, B. Lothenbach, The effect of temperature on the hydration of composite cements containing limestone powder and fly ash, Mater. Struct. 45 (2012) 1101–1114, https://doi.org/10.1617/s11527-011-9819-5.